Ordering process in the induction period of crystallization of poly(ethylene terephthalate)

M. Imai
Institute for Solid State Physics, University of Tokyo, Tokai-mura, Naka-gun, Ibaraki-ken, 319-11, Japan

K. Kaji and T. Kanaya
Institute for Chemical Research, Kyoto University, Uji, Kyoto-fu 611, Japan

Y. Sakai
Research Center, Toyobo Co. Ltd., Otsu, Shiga-ken 520-02, Japan

(Received 14 November 1994; revised manuscript received 1 May 1995)

Based on experimental findings, a mechanism of structural formation during the induction period of polymer crystallization is proposed. Recently we have found that, during the induction period of crystallization of poly(ethylene terephthalate) before crystal nuclei are produced, a correlation peak appears in small-angle x-ray scattering, and grows in intensity and position with time while the crystallization temperature is kept constant. The position of this peak is of course different from that of the intercrystallite correlation peak, the so-called long-period peak, in the crystallization stage; the former peak position is considerably lower than the latter. Surprisingly the time evolution of the former peak obeys the spinodal decomposition kinetics. In this study the cause for such a phenomenon is investigated from the viewpoint of the orientation fluctuations of rigid molecular segments using depolarized light scattering as well as small-angle neutron scattering (SANS). The depolarized light-scattering measurements indicate that during the induction period the parallel ordering of the rigid molecular segments occurs and this ordering process agrees with the spinodal decomposition kinetics in the isotropic-nematic transition theory proposed for stiff polymers by Doi *et al.* Further, the critical concentration of rigid segments at which the isotropic state becomes unstable is discussed using the molecular stiffness or the persistence length estimated from the molecular conformations observed by an isotope-labeling method for SANS.

I. INTRODUCTION

In crystallization it is an unquestionably important problem how crystal nuclei are formed. Kinetic and thermodynamic studies on crystal nucleation[1] have been made extensively based on the concept that crystallization is one of the first-order phase transitions which can be initiated by localized fluctuations of some order parameter such as density. When these fluctuations are larger than some critical size, nucleation starts. In recent years, however, the induction period of crystal nucleation, which is defined as a characteristic waiting time until nucleation starts, has been noted in the field of metallic,[2–6] inorganic,[7] and colloidal[8] systems. For example, Sutton *et al.*[5] performed *in situ* studies of the isothermal crystallization of an amorphous alloy of $NiZr_2$ using a time-resolved wide-angle x-ray diffraction (WAXD) and found that the crystallization proceeds via a transient structural precursor. In the case of the martensitic transition, Abe *et al.*[6] studied the martensitic transition in In-Tl alloys using WAXD and wide-angle neutron-diffraction (WAND) techniques and found that during the induction period of this martensitic transition a dynamic embryo, having a structure somewhat distorted from the low-temperature phase, appears and after the dynamic embryo grows to a critical size, it becomes a static nucleus having the same structure as the low-temperature phase. These results suggest that a pretransition structure appears in the induction period of first-order phase transitions, but the kinetics in the induction period has not been clarified as yet, neither experimentally nor theoretically.

In the case of crystallization of polymers consisting of linear chain molecules, the induction period is the stage when randomly entangled polymer chains transform to the regular aligned lattice. Because of topological obstruction of such entanglements, the polymer crystallization is extremely slow. This makes it easy to observe the structural change during the induction period.

Recently, we[9,10] investigated the structural formation in the induction period of the crystallization of poly(ethylene terephthalate) (PET) using WAXD and small-angle x-ray-scattering (SAXS) techniques. Here we show the feature of

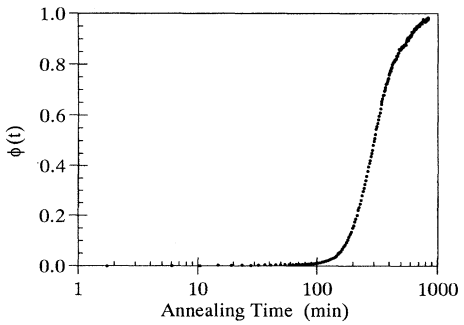

FIG. 1. Crystallization isotherm of the PET sample annealed at 80 °C.

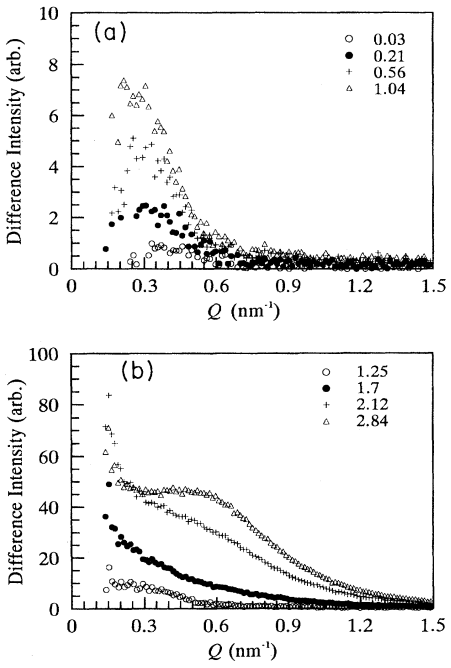

FIG. 2. SAXS profiles of the PET sample annealed at 80 °C from the glassy state as a function of reduced annealing time. The difference intensity means the observed intensity after subtraction of that for the melt-quenched sample.

the induction period observed in this system. Figure 1 shows the crystallization isotherm $\phi(t)$ for the annealing process of PET at 80 °C. During the initial annealing time of about 100 min, $\phi(t)$ does not change from the initial value, indicating the induction period. After that, $\phi(t)$ increases rapidly with annealing time, which indicates the initiation of crystallization. The time evolution of SAXS profiles in difference intensity during this annealing process is reproduced in Fig. 2 where reduced annealing time τ, defined by

$$\tau = \frac{t}{t_0}, \tag{1}$$

was introduced, t and t_0 being the annealing time and induction period, respectively. The difference intensity was obtained by subtracting the intensity of the melt-quenched amorphous sample from those of annealed samples. It is noted that during the induction period the scattering intensity profile shows a maximum, and as the annealing time increases, the maximum position shifts toward smaller Q while the maximum intensity increases. After the induction period, another scattering peak appears near $Q=0.6$ nm^{-1} and increases in intensity with annealing time. The latter is a well-known, so-called long-period peak due to the formation of lamellar crystals.

These results indicate that the density fluctuations, having a characteristic wavelength, occur before formation of critical crystal nuclei because it was confirmed from the WAXD measurements[9] that no short-range ordering is observed in the induction period. According to a detailed study,[10] the ordering process in the induction period could be divided into two stages, the early and late stages. In the early stage, the scattering maximum position did not move with annealing time and the scattering behavior could be described by Cahn's linearlized theory for spinodal decomposition.[11] In the late stage, the scattering maximum position shifted toward smaller Q with increasing maximum intensity and the scattering behavior could be described in terms of Furukawa's scaling theory.[12] Surprisingly, this growing process of the density fluctuations is thus very similar to that of spinodal decomposition in phase separation. Then the next step is to understand what the nature of the induction period of crystallization is.

Concerning the polymer crystallization problem, Flory[13] studied the statistical thermodynamics of semiflexible chain molecules in the crystallization using a lattice dynamics and proposed the following two-step crystallization model: First, cooperative ordering of the chains in a given region into a parallel alignment occurs without changing intermolecular interactions, and then longitudinal adjustment occurs, resulting in the more efficient packing of the chains in the parallel state to increase intermolecular interactions. We have considered that the first nematic transition process probably corresponds to the structural formation in the induction period. Recently, the dynamics of the isotropic to nematic transition was investigated theoretically by Doi and co-workers.[14–16] Doi and co-workers have shown that the behavior of spinodal decomposition occurs in the formation process of the liquid crystalline phase of stiff polymers (see Sec. II). These works are instructive when we interpret the time evolution of the SAXS profiles observed in the induction period of crystallization. In a preceding letter,[17] we reported that the orientation fluctuations play a very important role in the ordering process in the induction period. The purpose of this study is to investigate the ordering process in the induction period of crystallization from the viewpoints of orientation fluctuations and chain conformation. For this purpose we have performed time-resolved measurements of depolarized light scattering and small-angle neutron scattering (SANS) for the annealing process of PET.

II. THEORETICAL BACKGROUND

Doi and co-workers[14–16] have investigated the dynamics of the formation of the liquid crystalline phase of stiff polymers using a kinetics of two order parameters of concentration and orientation and have shown the following kinetic equation:

$$\frac{\partial f}{\partial t} = \frac{\partial}{\partial \mathbf{r}}[D_{\parallel}\mathbf{uu} + D_{\perp}(\mathbf{I}-\mathbf{uu})]\left[\frac{\partial f}{\partial \mathbf{r}} + f\frac{\partial}{\partial \mathbf{r}}W\right] + D_r\mathscr{R}[\mathscr{R}f + f\mathscr{R}W]. \tag{2}$$

Here $f(\mathbf{r},\mathbf{u},t)$ is the distribution function or the probability of finding a polymer parallel to the unit vector $\mathbf{u}$ at time t and a position $\mathbf{r}$, $\mathbf{I}$ is the unit tensor, W denotes the excluded volume type of potential between rods, $D_{\parallel}$ and $D_{\perp}$ are the translational diffusion constants parallel and perpendicular to the rod axis, respectively, D_r is the rotational diffusion con-

stant, and $\mathscr{R}$ is the rotational operator defined by $\mathbf{u}\times(\partial/\partial\mathbf{u})$. The orientation fluctuations $S_{\mathbf{Q}\alpha\beta}$ in the α-β plane can be defined by

$$S_{\mathbf{Q}\alpha\beta}=\int d\mathbf{u}\, f_{\mathbf{Q}}(\mathbf{u},t)(u_\alpha u_\beta-\tfrac{1}{3}\delta_{\alpha\beta}), \tag{3}$$

where $f_{\mathbf{Q}}(\mathbf{u},t)$ is the Fourier component of $f(\mathbf{r},\mathbf{u},t)$. When we assume that the polymer can move only along the chain axis, i.e., $D_\perp=D_r=0$, and orientation fluctuations proceed by three kinds of modes, so-called twist, bend, and splay. Of these modes the splay mode is coupled with density fluctuations, which provides an explanation for the fact that the orientation ordering process involves density fluctuations, which have been observed by SAXS. As the kinetic equations for these modes assume a similar form, only the equation for the bend mode is, for example, given:

$$\frac{\partial S_{Q\ \text{bend}}}{\partial t}=-\frac{D_\parallel}{7L^2}\left[12\left(1-\frac{\nu}{\nu^*}\right)K^2+\frac{25\nu}{9\nu^*}K^4\right]S_{Q\ \text{bend}}, \tag{4}$$

with

$$\mathbf{K}=\mathbf{Q}L/2.$$

Here ν is the concentration of rodlike segments and ν^* is the critical concentration at which the isotropic liquid becomes unstable:

$$\nu^*=\frac{16}{\pi dL^2}, \tag{5}$$

L and d being the length and diameter of the rod, respectively. Equation (4) corresponds to the differential equation describing the spinodal decomposition given by Cahn.[11] Thus, when $\nu>\nu^*$, the isotropic system becomes unstable and the fluctuation amplitude with a characteristic length grows exponentially with time. It is therefore expected that the exponential growth of the orientation fluctuations due to the parallel ordering of polymer segments can be observed experimentally. Such a result is the same as in cases of the other two modes. Then we can observe the behavior of spinodal decomposition when the system satisfies the $\nu>\nu^*$ condition. In order to investigate the ordering process in the induction period on the basis of this nematic transition theory, it is necessary to confirm the orientational ordering occurring in the induction period and examine it in terms of the critical condition given by Eq. (5).

III. ANALYTICAL METHODS

The orientation fluctuations can be detected using the depolarized light-scattering technique. For the analysis of the scattering from solids in which orientation fluctuations are randomly correlated, a statistical approach, developed by Stein and co-workers,[18,19] was employed. The Rayleigh factor $R_\perp(Q)$ for depolarized light scattering for such a system can be expressed by

$$R_\perp(Q)=\left(\frac{\omega}{c}\right)^4\frac{\langle\delta^2\rangle}{15}\int_0^\infty g(r)\frac{\sin(Qr)}{Qr}(4\pi r^2)dr, \tag{6}$$

where Q is the magnitude of the scattering vector, ω is the angular frequency of incident radiation, c is the velocity of light, $\langle\delta^2\rangle$ is the mean-square anisotropy, and $g(r)$ is the function of orientation defined as $g(r)=(3\langle\cos\phi_{i,j}\rangle_r-1)/2$, where $\phi_{i,j}$ is the angle between the optical axes of the ith and jth elements. The total integrated intensity or the invariant for contribution due to the orientation fluctuations I_{orient} can be expressed by

$$I_{\text{orient}}=\int_0^\infty R_\perp(Q)Q^2dQ=\frac{2\pi^2}{15}\left(\frac{\omega}{c}\right)^4\langle\delta^2\rangle. \tag{7}$$

When we consider this orientation ordering process, the criterion of Doi and co-workers plays an important role. In order to examine the critical condition, it is necessary to estimate the length of the rodlike segment or the stiffness of the chain. As the stiffness of the chain, we employed the so-called persistence length, which can be obtained from the single-chain scattering function. In general, a polymer chain in the amorphous state can be represented by the Kratky-Porod or wormlike chain model which describes a continuous transition from a Gaussian coil to an infinitely thin rod with increasing Q.[20,21] Three different analytical models have been proposed to describe the scattering function for the unperturbed Kratky-Porod chain. Yoshizaki and Yamakawa[21,22] have developed the scattering function describing the low-Q range corresponding to the Gaussian coil region, which is inapplicable to the determination of the persistence length. Des Cloizeaux[21,23] has given the exact scattering function in a series expansion for the infinitely long chain, which is valid only in the high-Q range, corresponding to the rod part for the real finite chain. In principle, the limiting form of this function for $Q\to\infty$ seems to be sufficient for the estimation of the persistence length. Practically, however, the fit with the limited observed data involved a considerable uncertainty owing to the usual experimental error. In the present study, where the slight change of the persistence length is required to be detected, this function could not be used. On the other hand, Sharp and Bloomfield have obtained the scattering function for the unperturbed wormlike chain as as special case for the wormlike chain with perturbation (excluded volume) effects, in a simple analytical form for a wide Q range containing both the coil and rod regions. It is confirmed that this function agrees well with the des Cloizeaux's function for $Q\to\infty$.[21] We therefore employed the function of Sharp and Bloomfield, which could be well fitted with the whole observed data as will be shown later, providing considerably reliable persistence length.

The scattering function developed by Sharp and Bloomfield[21,24] is expressed as

$$I_n(Q)=\frac{2(e^{-x}+x-1)}{x^2}+\left[\frac{8}{15}+\frac{14}{15x}-\left(\frac{22}{15}+\frac{14}{15x}\right)e^{-x}\right]\times\left(\frac{M_L}{M}\right)a, \tag{8}$$

with

$$x=\frac{L_c a Q^2}{3}, \tag{9}$$

where M is the molar mass of the polymer, $I_n(Q)$ is the single-particle scattering function, normalized in such a way that $I_n(0)=1$, and $M_L=M_0/p_0$ (M_0 is the molar mass of the monomer unit, and p_0 is the pitch of the monomer unit in the extended chain conformation). We estimated the persistence length a by fitting Eq. (8) to the single-chain scattering data obtained from small-angle neutron-scattering measurements and examined the criterion of Doi and co-workers given by Eq. (5).

IV. EXPERIMENT

A. Samples

For the depolarized light-scattering measurements, we used PET pellets presented from Toyobo Co. Ltd.[9] This PET sample has a number-average molecular weight M_n of 25 000 and a polydispersity $M_w/M_n=2.5$. The glass transition temperature T_g and the melting temperature T_m of this sample were 75 and 250 °C, respectively. This PET sample contains only 30 ppm phosphor and 30 ppm germanium as additives in order to reduce the excess scattering from impurities.

For the SANS measurements, both deuterated and hydrogenated PET's (D-PET and H-PET) were synthesized by transesterification of dimethylterephthalate and ethylene glycol followed by polycondensation. As deuterated dimethyl terephthalate was not commercially available, it was synthesized from deuterated terephthalic acid and methanol. The obtained deuterated dimethyl terephthalate was then purified by recrystallizing twice from the methanol solution. For the transesterification, we used 0.03 mol % zinc acetate and 0.04 mol % Sb_2O_3 as catalysts. The molecular weights of both the deuterated and nondeuterated PET were determined to be $M_n=17\,000$ and 21 500, respectively, by viscosity measurements in a phenol and tetrachloroethane mixture. Both samples also had nearly the same T_g and T_m of 75 and 250 °C, respectively.

B. Depolarized light scattering measurements

The PET sample was melted at 290 °C for 2 min and immediately thereafter quenched in ice water. The density of the melt-quenched sample was 1.333 g/cm^3, which agrees with the value reported for the amorphous PET,[25] and no crystalline diffraction peaks were observed in the wide-angle x-ray scattering profiles for this sample. The isothermal annealing of the amorphous samples was performed at 80 °C within 0.1 °C on a hot stage for optical microscopes (Linkam 600 T). The annealing process was followed by the time-resolved depolarized light-scattering measurements. We paid special attention to the purity of the sample and the optical parts to reduce the background scattering. We used a plane-polarized He-Ne laser beam ($\lambda=633$ nm). The beam was passed through a two-aperture system to eliminate parasitic scattering. The sample on the hot stage was irradiated by the beam, and the scattered light intensity was recorded by a 38-photodiode-array system having a wide detector area. The scattering measurements were carried out under H_V (depolarized) optical geometry. In order to detect the weak intensity change, exposure time was taken to be 2 s and the measurements were performed several times to check the reproducibility.

C. SANS measurements

In order to obtain the single-chain scattering function, we used diluted mixtures of 95 wt. % D-PET and 5 wt. % H-PET.[26] This is because we need to obtain the single-chain scattering function up to a fairly high-Q range ($Qa\sim4$) in order to estimate the persistence length,[21] and this low amount of H-PET reduces the incoherent scattering from H nuclei which interferes with the evaluation of single-chain scattering function especially in the rather high-Q region. D-PET and H-PET were blended by dissolving in a common solvent of hexafluoro-2-propanol and then reprecipitating in methanol. The precipitate was dried in a vacuum oven and melt pressed under nitrogen atmosphere for 2 min at 285 °C. This melt condition was determined from the optimum condition to eliminate the so-called memory effect of polymer crystallization and to prevent the transesterification between D-PET and H-PET. Immediately after the melt press, the sample was quenched in ice water to prevent crystallization. The density of the melt-quenched blend sample was observed to be 1.388 g/cm^3, and no crystalline peaks were observed in the WAXD profiles for this sample. The sample may have changed to a H-D block copolymer as a result of the transesterification during the melt-press process, but this problem will be discussed later in Sec. VII. The amorphous melt-quenched blend sample was annealed for various given times at 88 °C in an oil bath and then quenched into ice-cold water to fix their states. At this annealing temperature we can neglect the transesterification reaction between hydrogenated and deuterated PET.[27] Amorphous samples of pure D-PET and pure H-PET were also prepared for estimation of inhomogeneities of the pure PET structure itself and incoherent scattering. The sample thicknesses of D- and H-PET were adjusted so that they would correspond to the blend ratio. These samples were also annealed and quenched under the same conditions as the blend sample. SANS measurements were performed at room temperature for the quenched samples. This annealing process was also followed by the density measurement to obtain the crystallization isotherm.

The SANS measurements were performed using a SANS instrument of the Institute for Solid State Physics of the University of Tokyo (SANS-U) at the JRR-3M reactor of the Japan Atomic Energy Research Institute (Tokai).[28] In the SANS-U instrument, a two-dimensional position-sensitive detector with 650×650 mm^2 area, having 5×5 mm^2 resolution, was positioned at two sample-to-detector distances of 1 and 4 m. As all the measurements were performed at the wavelength λ of 0.7 nm with resolution $\Delta\lambda/\lambda=0.1$, the covering Q range was 0.08–3.5 nm^{-1}.

D. SANS data reduction

The obtained two-dimensional scattering patterns from the blend specimens were circularly averaged to obtain the one-dimensional scattering function $I(Q)$ because the scattering patterns showed cylindrical symmetry. The scattering data were then corrected for instrumental background, detector efficiency, transmission, and specimen thickness. The scattering intensities from H-PET and D-PET were used for estimation of incoherent scattering intensity from H and D nuclei and structural scattering arisen from inhomogeneities of bulk PET. After these corrections, the scattering functions

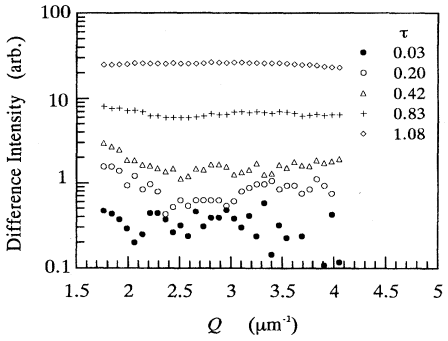

FIG. 3. Depolarized light scattering profiles of the PET sample annealed at 80 °C from the glassy state as a function of reduced annealing time.

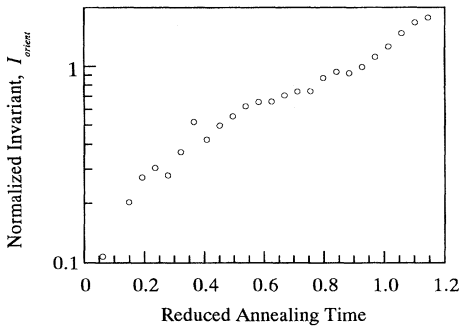

FIG. 4. Annealing time dependence of the invariant for orientation fluctuation I_{orient} obtained from the time-resolved DLS measurement at 80 °C.

were converted to absolute differential scattering cross sections $d\Sigma(Q)/d\Omega$ by comparison with the scattering intensity of the standard sample Lupolen which is calibrated against standard vanadium.[29] Then we can get the differential scattering cross section for hydrogenated block. For a mixture of H- and D-PET without any specific interaction, the differential scattering cross section per unit volume is given by[26]

$$\left[\frac{d\Sigma(Q)}{d\Omega}\right]_{\text{label}} = c_{\text{H}}(1-c_{\text{H}})n_w K I_n(Q), \tag{10}$$

where c_{H} is the concentration of hydrogenated segments, n_w is the degree of polymerization, and K is the contrast factor given by

$$K = \frac{\rho N_L}{M_0}(m|b_{\text{D}} - b_{\text{H}}|)^2, \tag{11}$$

with ρ=density, N_L=Avogadro number, M_0=monomer molecular weight, $b_{\text{D}}, b_{\text{H}}$=scattering lengths of deuterium or hydrogen, and m=number of exchanged hydrogen nuclei per monomer. In Eq. (10) n_w means the degree of polymerization of the block and $I_n(Q)$ is the single-chain scattering function for a hydrogenated block:

$$I_n(Q) = \frac{1}{n_w^2}\left\langle \sum_{i,j} \exp[iQ(R_i - R_j)] \right\rangle. \tag{12}$$

Here we neglect the cross term characterizing the interference between the D and H parts of the same molecule as a consequence of transesterification for an intermediate-Q range.[30,31] The obtained $I_n(Q)$ were analyzed on the basis of the scattering function for the wormlike chain proposed by Sharp and Bloomfield.[21,24]

V. ORIENTATION FLUCTUATIONS IN THE INDUCTION PERIOD OF CRYSTALLIZATION

As described in the Introduction, orientation fluctuations may play a very important role in the structure formation during the induction period. In this section, we confirm the role of the orientation fluctuations occurring in the induction period of crysallization by means of a depolarized light-scattering technique.

Figure 3 shows the semilogarithmic expression of time evolution of the depolarized light-scattering intensity in the early stage of the annealing process of the sample at 80 °C as a function of Q from which the depolarized intensity of the unannealed sample was subtracted. This annealing condition was the same as that of the SAXS measurements described in the Introduction. During the induction period, the scattering profiles are almost independent of Q and the scattering intensity increases with annealing time. Figure 4 shows the time dependence of the invariant I_{orient} for orientation fluctuations in a semilogarithmic scale, which was calculated by Eq. (7). Here I_{orient} is normalized as $I_{\text{orient}}(\tau=1)=1$. The invariants appear to increase almost exponentially with annealing time until $\tau=0.5$, but between 0.5 and 1.0, it levels off somewhat. After the induction period, the rate is suddenly accelerated and the invariant increases exponentially again, which is due to the formation of spherulite texture. The exponential increase of I_{orient} agrees with the prediction of the theory of Doi and co-workers, suggesting that the parallel ordering actually occurs during the induction period. The two-step ordering process is also consistent with the SAXS results, indicating early and late stages in the induction period.

In the following we discuss the critical concentration ν^* defined by Eq. (5). The PET molecule is composed of rigid terephthalate groups and soft ethylene groups; in other words, it consists of rigid rod segments connected by the flexible parts. The problem is whether or not such rod segments really satisfy the criterion of Doi and co-workers. In order to examine the criterion, we estimated the value of the length L and the diameter d of the rod in the amorphous state as follows. As an approximate value of L, we adopted the persistence length in the wormlike chain model. Gonzalez *et al.*[32] reported that the persistence length of a PET molecule in the θ state is 1.2 nm. This value almost corresponds to the monomer unit length of 1.08 nm. For the cross-sectional diameter of the rod, we took the van der Waals width of a benzene ring of 0.66 nm because it is considered that the benzene ring is freely rotating around the molecular axis just above the glass transition temperature.[33] Using these values for the calculation, we get a critical concentration ν^* of 5.4 segments/nm^3. The concentration ν of PET segments at a given temperature can be calculated from the density at that temperature and the mass of the segment.

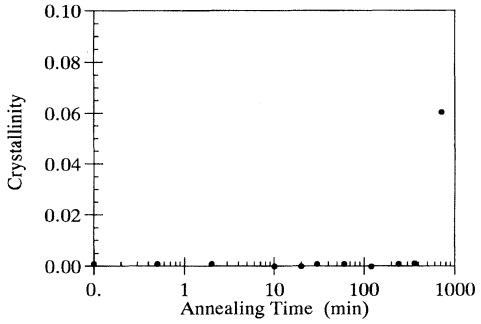

FIG. 5. Annealing time dependence of crystallinity (crystallization isotherm) for the D-PET sample used for SANS measurement at 88 °C. The crystallinity was obtained by density measurements.

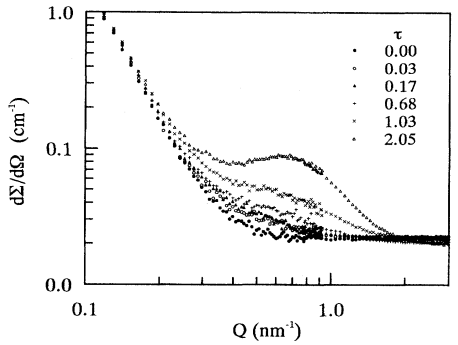

FIG. 6. SANS profiles of the D-PET sample annealed at 88 °C from the glassy state as a function of reduced annealing time.

Since the density of the glassy PET is 1.333 g/cm^3 and the mass of a monomer is 192 g/mol, the concentration of the segment in the glassy state is estimated to be 4.2 segments/nm^3, resulting in $\nu < \nu^*$. In the glassy or melt state of PET, we therefore cannot observe the orientation ordering or liquid crystalline state. However, we consider the following scenario for the structure formation in the induction period of crystallization. When PET is annealed above the glass transition temperature, the internal rotation of ethylene groups begins to be allowed due to the release from the frozen state and the most stable chain conformation of the trans form is preferred to the gauche one. For example, in the case of n-butane the trans conformation is about 3.35 kJ/mol more stable than the gauche one.[34] This conformational change increases the length of the rod segments. When the conformation of one of two CH_2 groups per monomer changes from gauche to trans as an average, it is expected that the rod length becomes 0.25 nm longer than that in the glassy state because the two CH_2's repeating unit has a length of 0.25 nm. This increase of the rod length leads to the decrease of the critical concentration to a value of 3.7 segments/nm^3. In this case, the condition $\nu > \nu^*$ is achieved and the isotropic state becomes unstable. Then the phase transition from the isotropic to the orientationally ordered state occurs following the kinetics of spinodal decomposition. Therefore, the key point of this scenario is to confirm the increase of the chain stiffness parameter such as the persistence length in the induction period of crystallization.

VI. DENSITY FLUCTUATIONS IN THE INDUCTION PERIOD OF CRYSTALLIZATION EXAMINED BY SANS

In order to examine the change of the chain stiffness, we employed the time-resolved SANS measurements for the annealing process of the D- and H-PET mixture. Before going on to the study of the chain stiffness, we follow the behavior of density fluctuations in the induction period of crystallization of D-PET at 88 °C. Figure 5 shows the crystallization isotherm for D-PET obtained by the density measurement. The volume fraction of crystallinity of the sample was obtained by the relation

$$X_c = (\rho - \rho_a)/(\rho_c - \rho_a), \tag{13}$$

where ρ, ρ_c, and ρ_a represent the densities of the sample, the crystalline part (1.516 g/cm^3), and the amorphous part (1.389 g/cm^3), respectively. Here we estimated the density of the crystalline part for D-PET from the value of H-PET. From this isotherm, the induction period of this annealing process is obtained as about 300 min.

The growth process of the density fluctuations in the induction period of this annealing process was followed by time-resolved SANS measurement of the fully deuterated PET sample. Figure 6 shows the time evolution of SANS profiles for deuterated PET at 88 °C in a double-logarithmic expression. Despite the induction period of crystallization where the macroscopic density does not change from the amorphous one, the scattering intensity at around $Q = 0.5$ nm^{-1} increases with annealing time. After the induction period of crystallization, the scattering intensity increases rapidly and makes a scattering peak due to the so-called long-period structure, which corresponds to $\tau = 1.03$ and 2.05. In order to show the structural change in the induction period, we subtracted the intensity of the melt-quenched sample from those of the annealed samples. Figure 7 shows the difference scattering profiles for the samples during the annealing process. This figure shows that a scattering maximum appears at around $Q = 0.5$ nm^{-1} for $\tau = 0.03$. As the annealing time increases, the maximum position seems to shift to-

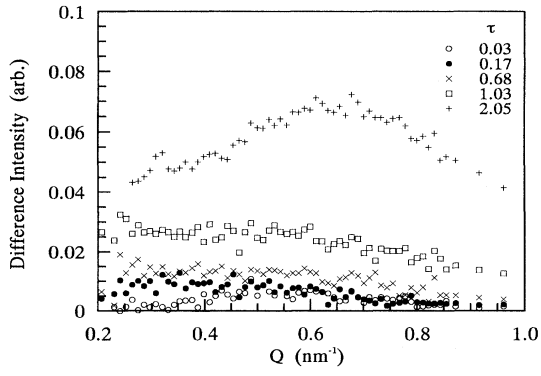

FIG. 7. SANS profiles of the D-PET sample annealed at 88 °C from the glassy state as a function of reduced annealing time. The difference intensity means the observed intensity after subtraction of that for the melt-quenched sample.

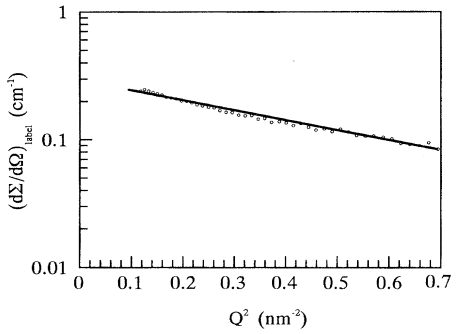

FIG. 8. Guinier plot of the melt-quenched H/D-PET blend sample.

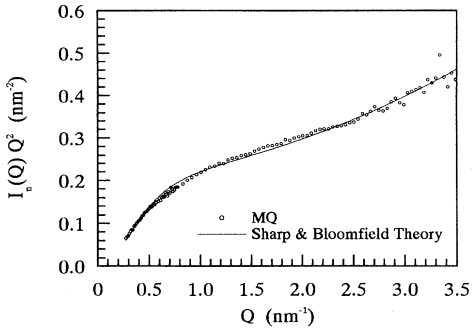

FIG. 9. Kratky plot of the melt-quenched H/D-PET blend sample. Drawn curve: best fit to the data using a scattering function for the wormlike chain proposed by Sharp and Bloomfield (Ref. 24).

ward smaller Q simultaneously with increasing the maximum intensity. After the induction period, the scattering intensity in the vicinity of $Q=0.7$ nm^{-1} begins to increase due to the appearance of the long-period structure. This time evolution of the scattering profiles in the induction period is very similar to the behavior of SAXS profiles as shown in Fig. 2. These results have reconfirmed the growth process of the density fluctuations in the induction period.

VII. CHANGE OF CHAIN STIFFNESS IN THE INDUCTION PERIOD OF CRYSTALLIZATION REVEALED BY SANS

Based on the isotropic to nematic transition theory proposed by Doi and co-workers, we have investigated the single-chain conformation in the induction period of crystallization. First, we examine the single-chain conformation of the melt-quenched sample in terms of the unperturbed chain model and then investigate the time evolution of the single-chain conformation in the induction period.

A. Single-chain conformation

Before we determine the single-chain conformation in the melt-quenched blend sample, we must solve the problem of transesterification occurring during the melt-quenching process. First, we evaluate the extent of transesterification by determining the average molecular weight M_w^b of hydrogenated blocks in the blend sample. For small-Q region, the single-chain scattering function $I_n(Q)$ may be approximated by

$$I(n(Q)\approx\exp(-\tfrac{1}{3}Q^2R_g^2), \tag{14}$$

where R_g is the radius of gyration. Since $I_n(0)=1$, $M_w^b=M_0n_W$ can be determined from the extrapolated value $[d\Sigma(Q)/d\Omega]_{\text{label}}$ of Eq. (10) with Eq. (11). Figure 8 shows the Guinier representation of the $[d\Sigma(Q)/d\Omega]_{\text{label}}$ for the melt-quenched blend sample, indicating that Eq. (14) is valid within experimental error. From the intercept at $Q=0$, $M_w^b=4650$ was obtained, suggesting about 90% reduction of molecular weight from the initial one. This reduction is due to the transesterification having occurred when the sample was melted for 2 min at 285 °C during the melt-quenching process. Kugler *et al.*[27] studied the transesterification in PET using SANS and reported the transesterification rate as a function of annealing temperature and annealing time. According to their results, it is expected that there will be about 95% reduction of the molecular weight when PET is melted at 280 °C for 2 min, which is almost consistent with our result. From the slope of the curve in Fig. 8, the z-average radius of gyration of the hydrogenated block, R_{gz}^b, was also evaluated to be 2.82 nm. The next problem is whether or not the chain conformation of the transesterificated blocks is the same as that of the original pure H-PET. The fundamental idea for such judgment is as follows. If the hydrogenated block conformation is unperturbed or Gaussian, then we may conclude it is the same as that of the original H-PET because it is established that the chain conformation in the amorphous bulk is unperturbed.[35,36]

The chain conformation in the H block can be estimated by determining the ratio of the weight-averaged radius of gyration R_{gw} to $M_W^{1/2}$, which is a measure of the unperturbed chain.[35] The R_{gz}^b obtained from Guinier analysis for the melt-quenched sample was 2.82 nm as described before. If we assume a Schultz-Flory distribution with a polydispersity $M_w/M_n=2$, which is reasonable for polycondensation polymers, it is possible to convert the z-average radius of gyration to a weight average value,[36] R_{gw}, by

$$R_{gw}^2=R_{gz}^2\frac{1+U}{1+2U}, \tag{15}$$

where U is the polydispersity $M_w/M_n-1=1$. Using Eq. (15), we obtained a value of 0.034 nm for the ratio of R_{gw} to $M_W^{1/2}$. Flory calculated the dimension of the unperturbed PET chain using a statistical model and obtained the ratio of 0.039 nm.[35] Our ratio was only slightly lower than the value predicted by Flory and agreed well with the value obtained experimentally by Gilmer *et al.*[36] of 0.032 nm. It is therefore concluded that the chain conformation of H blocks is unperturbed. The value of the ratio of R_{gw} to $M_W^{1/2}$ did not change during the induction period. Thus the important idea in this study is obtained that at least during the induction period of crystallization, the polymer chain remains to assume the unperturbed conformation and the local conformation or persis-

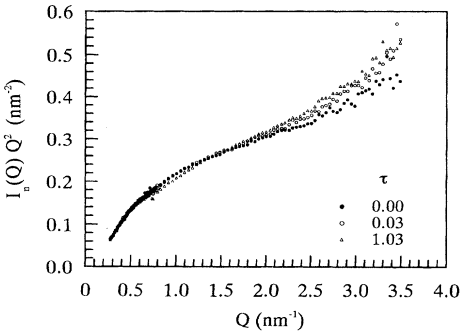

FIG. 10. Annealing time dependence of single-chain scattering function in a Kratky-plot expression.

tence length of the block chains is equal to that of the original pure PET. Based on this conclusion, we estimate the persistence length below.

A Kratky plot representation of the single-chain scattering function $I_n(Q)$ for the blocked melt-quenched sample is shown in Fig. 9. Here we corrected for the influence of the cross section of the chain using the scattering function for an infinitely long rod molecule given by

$$I_n(Q)=\frac{\pi M_L}{M}\frac{1}{Q}\exp\left(-\frac{Q^2r_0^2}{4}\right), \tag{16}$$

where r_0 is the radius of a rod. We fit the observed scattering profiles with the theoretical scattering function in the range of $a^{-1}<Q<r_0^{-1}$ and obtained the value of 0.28 nm for r_0, which is close to the van der Waals width of a benzene ring, 0.33 nm. The corrected single-chain scattering function in Kratky representation shows a plateau, indicating a Gaussian chain and a linear increase in the higher-Q range, indicating the rodlike nature of the chain. We fit the obtained scattering function by the calculated scattering function for the wormlike chain proposed by Sharp and Bloomfield.[24] Such a fit is also given in Fig. 9, and the obtained value for the persistence length is 1.22 nm. This persistence length agrees well with the reported value of about 1.2 nm obtained by hydrodynamic data in the θ condition.[32]

B. Time evolution of single-chain conformation

The change of the single-chain scattering function in the induction period is shown in Fig. 10 in a Kratky-plot expression. Qualitatively, the intersection of the two asymptotic scattering behaviors of Gaussian at low-Q range and rodlike at high-Q range leads to the persistence length. Then the persistence length seems to increase during the induction period of crystallization. However, this method is too simple to determine the annealing time dependence of the persistence length exactly; then, we fit the scattering functions by the wormlike chain model to obtain the persistence length. Figure 11 shows the annealing time dependence of the resulting persistence lengths during the induction period of crystallization. The persistence length appears to increase in the early stage of the induction period from 1.22 to 1.33 nm. After the initial increase it levels off, but in the end stage of the induction period it increases again to about 1.6 nm. This annealing time dependence of the persistence length agrees well with the prediction of our parallel ordering model.

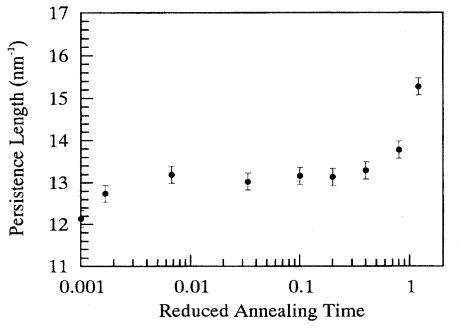

FIG. 11. Annealing time dependence of the persistence length.

VIII. DISCUSSION

In the following we make a somewhat quantitative discussion about the critical concentration ν^* defined by Eq. (5). As an approximate value of L, we adopted the persistence length in the wormlike chain model and for the cross-sectional diameter of the rod we took the van der Waals width of a benzene ring of 0.66 nm. In the case of the melt-quenched amorphous state, we get a critical concentration ν^* of 5.2 segments/nm^3 using $L=1.22$ nm and the concentration ν of 4.2 segments/nm^3, resulting in $\nu<\nu^*$. This result confirms our discussion in Sec. V. In the case of the early stage of the induction period, ν^* becomes 4.3 segments/nm^3 if we employ the observed average value of persistence length, 1.33 nm, as the rod length L. Such a decrease of ν^* from 5.2 segments/nm^3 may be considered to cause the phase transition to the orientationally ordered phase, but this ν^* is still lightly larger than that of $\nu=4.2$ segments/nm^3 for the amorphous PET sample. At the present stage, the reason for this is not clear though some factors in the theory can be considered. Anyway, the increase of the persistence length, which may be due to the conformational change from gauche to trans form, induces the parallelization of the polymer chains having the spinodal decomposition kinetics, and then longitudinal adjustment occurs, resulting in the more efficient packing of the parallel oriented chains to form a crystal nucleus. A similar spinodal decomposition due to the orientation fluctuations has been predicted by Brochard-Wyart and de Gennes[37] when the chain orientation is temporarily given by a rapid stretching.

IX. CONCLUDING REMARKS

Here we have reported an ordering process during the induction period of polymer crystallization, where two order parameters, density and orientation, play an important role. This suggests that under the conditions where polymers crystallize the amorphous state is not metastable, but unstable, and the parallel ordering of polymer segments occurs due to the increase of the polymer chain rigidity. This parallel or-

dering is a pretransition phenomenon, and after this ordering proceeds to a certain level, crystallization starts. Although it is yet unclear whether or not the existence of such pretransition structure is of universal nature, it has also been reported, as described in the Introduction, in the fields of metallic,[2–6] inorganic,[7] and colloidal[8] systems that the crystal nucleation proceeds through transient structural precursors.

ACKNOWLEDGMENTS

We would like to express our sincere thanks to Professor P. G. de Gennes of College de France for his interest and valuable comments. Thanks are also due to Dr. T. Sato, Department of Macromolecular Science, Osaka University, for helpful discussions.

[1] K. F. Kelton, in *Solid State Physics*, edited by H. Ehrenreich and D. Turnbull (Academic, New York, 1991), Vol. 45, p. 75.

[2] S. E. Nagler, R. F. Shannon, Jr., C. R. Harkless, and M. A. Singh, Phys. Rev. Lett. **61**, 718 (1988).

[3] R. F. Shannon, Jr., S. E. Nagler, C. R. Harkless, and R. M. Nicklow, Phys. Rev. B **46**, 40 (1992).

[4] Y. Noda, S. Nishihara, and Y. Yamada, J. Phys. Soc. Jpn. **53**, 4241 (1984).

[5] M. Sutton, Y. S. Yang, J. Mainville, J. L. Jordan-Sweet, K. F. Ludwig, Jr., and G. B. Stephenson, Phys. Rev. Lett. **62**, 288 (1989).

[6] H. Abe, M. Ishibashi, K. Ohshima, T. Suzuki, M. Wutting, and K. Kakurai, Phys. Rev. B **50**, 9020 (1994).

[7] N. Hamaya, Y. Yamada, J. D. Axe, D. P. Belanger, and S. M. Shapiro, Phys. Rev. B **46**, 7770 (1986).

[8] K. Shatzel and B. J. Ackerson, Phys. Rev. Lett. **68**, 337 (1992).

[9] M. Imai, K. Mori, T. Mizukami, K. Kaji, and T. Kanaya, Polymer **33**, 4451 (1992).

[10] M. Imai, K. Mori, T. Mizukami, K. Kaji, and T. Kanaya, Polymer **33**, 4457 (1992).

[11] J. W. Cahn, J. Chem. Phys. **42**, 93 (1965).

[12] H. Furukawa, Adv. Phys. **34**, 703 (1985).

[13] P. J. Flory, Proc. R. Soc. London A **234**, 60 (1956).

[14] T. Shimada, M. Doi, and K. Okano, J. Chem. Phys. **88**, 2815 (1988).

[15] M. Doi, T. Shimada, and K. Okano, J. Chem. Phys. **88**, 4070 (1988).

[16] T. Shimada, M. Doi, and K. Okano, J. Chem. Phys. **88**, 7181 (1988).

[17] M. Imai, K. Kaji, and T. Kanaya, Phys. Rev. Lett. **71**, 4162 (1993).

[18] R. S. Stein and P. R. Wilson, J. Appl. Phys. **33**, 1914 (1962).

[19] J. Koberstein, T. P. Russel, and R. S. Stein, J. Polym. Sci. Polym. Phys. Ed. **17**, 1719 (1979).

[20] O. Kratky and G. Porod, Rec. Trav. Chim. Pays-Bas **68**, 1106 (1949).

[21] R. G. Kirste and R. C. Oberthür, in *Small Angle X-ray Scattering*, edited by O. Glatter and O. Kratky (Academic, London, 1982), Chap. 12.

[22] T. Yoshizaki and H. Yamakawa, Macromolecules **13**, 1518 (1980).

[23] J. des Cloizeaux, Macromolecules **6**, 403 (1973).

[24] P. Sharp and V. A. Bloomfield, Biopolymers **6**, 1201 (1968).

[25] E. W. Fischer and S. J. Fakirov, J. Mater. Sci. **11**, 1041 (1976).

[26] E. W. Fischer, Makromol. Chem. Macromol. Symp. **20/21**, 277 (1988).

[27] J. Kugler, J. W. Gilmer, D. Wiswe, H. G. Zachmann, K. Hahn, and E. W. Fischer, Macromolecules **20**, 1116 (1987).

[28] Y. Ito, M. Imai, and S. Takahashi, Physica B (to be published).

[29] D. Schwahn and M. Imai, private collaboration using SANS-U and SANS at Julich. See also Ref. 28.

[30] H. C. Benoit and G. Hadziioannou, Macromolecules **21**, 1449 (1988).

[31] H. C. Benoit, E. W. Fischer, and H. G. Zachmann, Polymer **30**, 379 (1989).

[32] C. González, F. Zamora, G. M. Guzamán, and L. M. Química-Física, J. Macromol. Sci. Phys. B **26**, 257 (1987).

[33] R. Gehrke, M. Gulibrzuch, A. Klaue, and H. G. Zachmann, A. C. S. Polym. Prepr. **29**, 64 (1988).

[34] H. Tadokoro, *Structure of Crystalline Polymers* (Wiley, New York, 1978).

[35] P. J. Flory, *Statistical Mechanics of Chain Molecules* (Wiley-Interscience, New York, 1969).

[36] J. W. Gilmer, D. Wiswe, H. G. Zachmann, J. Kugler, and E. W. Fischer, Polymer **27**, 1391 (1986).

[37] F. Brochard-Wyart and P. G. de Gennes, C. R. Acad. Sci. Paris II **306**, 699 (1988).